https://doi.org/10.20965/ijat.2025.p0162

Technical Paper:

Development of an Application for Smartphone to Detect Chattering Vibration in Single-Purpose Lathe

Yoshihiro Makimoto[*,†], Yuya Nara[*], Syuma Hirai[**], Akira Mizobuchi[**], Yuki Oe[*], and Hitoshi Ogawa[*]

[*]Tokushima Prefectural Industrial Technology Center
11-2 Nishibari, Saika-cho, Tokushima, Tokushima 770-8021, Japan
[†]Corresponding author, E-mail: makimoto@itc.pref.tokushima.jp
[**]Tokushima University, Tokushima, Japan
[Received September 26, 2024; accepted December 5, 2024]

This paper proposes a novel chattering vibration detection application (CVDA) for smartphones. The main target machine is a single-purpose lathe. The CVDA uses sound signals between 10 kHz and 20 kHz, and acceleration sensor signals. In general, when evaluating chattering vibration detection methods using sound signals, it is necessary to consider that the operating sound of the target lathe includes environmental and other machine tool operating noise. The environmental noise includes human voices, the sound of rain, and factory broadcasts. The frequencies of these sounds are often less than 10 kHz. However, the operating sound of machine tools contains sound signals between 10 kHz and 20 kHz. In this study, a method to detect chattering vibrations was employed using sound signals between 10 kHz and 20 kHz to remove environmental sounds, and acceleration sensor data to remove the operating sounds of machine tools. The basic device of the proposed analyzer is a smartphone. The advantages of using a smartphone include compactness, convenience, and applicability to many factories.

Keywords: chattering vibration, sound signal, acceleration sensor data, fast fourier transform, smartphone

1. Introduction

Manufacturing industries require high production efficiencies. Chattering vibrations are one of major problems encountered during the cutting process. Various methods have been developed to predict and prevent chattering vibrations on machined surfaces [1–7]. However, there are problems such as the difficulty of integrating the system into existing systems. Therefore, various methods have been considered for abnormality detection and condition monitoring using sound signals. These methods can be easily incorporated into existing systems by installing a microphone [8–15]. Although anomaly detection systems using deep learning have high accuracy, there are issues such as the need for a large amount of teacher data for tuning and the high cost. The cost-effectiveness of this method remains unclear for companies. Thus, the purpose of this study is to develop an inexpensive and high-accuracy chattering vibration detection system for a single-purpose lathe. We propose an application for smartphones to detect chattering vibrations. The number of devices can be reduced because smartphones are equipped with sound sensors, acceleration sensors, camera functions, and a CPU as a standard. As smartphones are not designed for frequency analysis, their microphone characteristics are unknown. Therefore, we conducted an experiment to compare the smartphone and measurement microphone.

In this paper, the main target machine is a single-purpose lathe. The single-purpose lathe was off-the-shelf, and the workpiece was properly fixed. In contrast, the tool change and length of the tool adjustment were performed by workers. Chattering vibration may occur owing to loose tool fixturing or increased tool protrusion length because the adjustment is performed according to the worker's sense. The chattering vibration detection application (CVDA) is intended to compensate for the worker's sense. In this study, a carbon-steel turning experiment was conducted. To date, cutting sound waveforms have been investigated by turning carbon steel [8–10, 16–19]. However, intensive studies on the relationship between chattering vibrations and cutting sound signals at 10–20 kHz have not been conducted intensively. Thus, we measured the change in sound pressure between 10 and 20 kHz to vary the tool protrusion length. Chattering vibrations occurred when the tool protrusion length was increased, and we confirmed that the sound pressure between 10 and 20 kHz increased.

Next, we describe an application for detecting the chattering vibrations. This application can detect chattering vibrations by changes in cutting sounds. To date, the process and tool states have been investigated using cutting sounds [11]. However, the distinction between the target machine and noise is an issue with this the method because it detects loud sounds below 10 kHz. The sounds are environmental noise and other machine tool operating noise. Environmental noise in factories include human voices and broadcast sound. The frequencies of the noise sounds are generally less than 10 kHz [20]. By using sound signals

Table 1. FFT conditions.

Device	Sampling [Hz]	Points
Measurement microphone	25600	6400
Smartphone	44100	4096

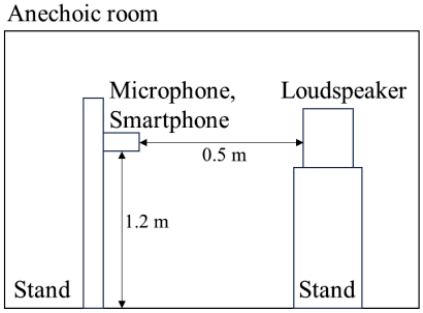

(a) Evaluating the characteristic of measurement microphone and smartphone microphone

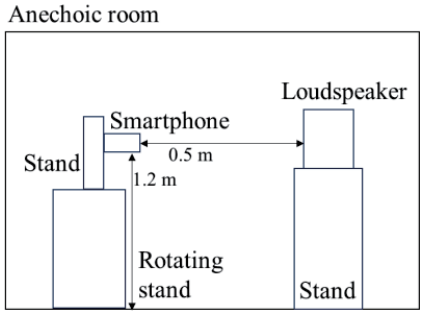

(b) Evaluating the directivity

Fig. 1. Setup for evaluating the characteristic of smartphone microphone.

between 10 and 20 kHz, chattering vibrations can be detected even in the presence of human voices and rain noise. Furthermore, an acceleration sensor was used to detect the start and end times of the cutting process based on the movement of the single-purpose lathe, and the sound was collected during the cutting process. False positives can be reduced even if noise, such as other machine tool sounds, are generated outside the cutting process time. Cutting experiments were performed by broadcasting noise sounds to confirm the detection of chattering vibration.

2. Microphone Characteristic Evaluation

2.1. Experimental Setup

In this section, we describe an experiment to evaluate the microphone characteristics of a smartphone (Zenfone8, ASUSTeK Computer Inc.) using a measurement microphone (4939-a-011, Bruel & Kjær Sound & Vibration Measurement A/S). The frequency response of the measurement microphone between 10 Hz and 20 kHz was flat. The general purpose speaker was utilized. **Table 1** lists the fast Fourier transform (FFT) conditions. **Fig. 1(a)** shows a schematic of experimental setup used to evaluate the characteristics. A loudspeaker was placed at a height

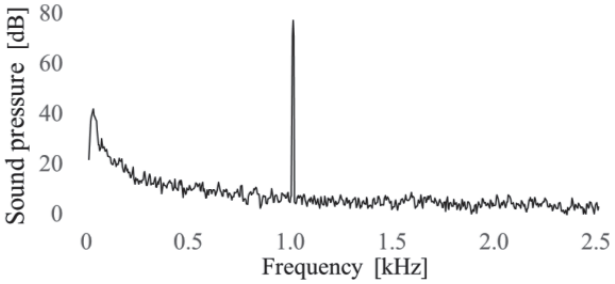

(a) 1 kHz sine wave detected by measurement microphone

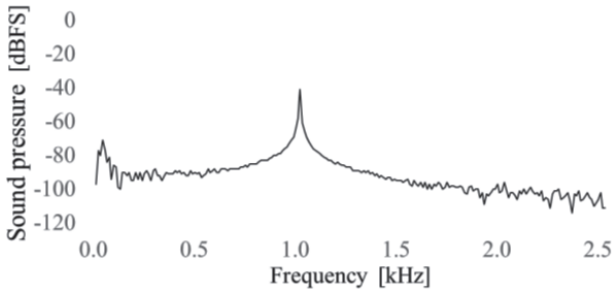

(b) 1 kHz sine wave detected by smartphone microphone

Fig. 2. Frequency spectrum chart of measurement microphone and smartphone microphone.

of 1.2 m in an anechoic room. The calibrated measurement microphone and smartphone were placed side by side 0.5 m in front of the loudspeaker. The loudspeaker emits a sine wave at a specific frequency. The frequencies selected were as follows: 125 Hz, 250 Hz, 500 Hz, 1000 Hz, 2000 Hz, 4000 Hz, 8000 Hz, and 16000 Hz. The microphone and smartphone measurements were performed simultaneously and their results were compared.

Next, we describe an experiment for evaluating the directivity of a smartphone microphone. **Fig. 1(b)** shows a schematic of the experimental setup for evaluating the directivity. The loudspeaker and smartphone were placed in an anechoic room. The loudspeaker emitted a sine wave at 16000 Hz, and the change in sound pressure was measured while the smartphone was rotated 0°, 30°, 60°, 90°, 120°, 150°, 180°, 210°, 240°, 270°, 300°, and 330°.

2.2. Experimental Result Comparing Microphone and Smartphone and Discussion

Figure 2 shows a frequency spectrum chart of a sine wave at 1.0 kHz measured by measurement microphone and smartphone microphone. The frequency of the highest sound pressure was 1000 and 1001 Hz for the measurement and smartphone microphones, respectively. The sound pressure of the measurement microphone was −77.2 dB, while the sound pressure of smartphone microphone was −41 decibel full scale (dBFS). The sound pressure difference between 1.0 kHz and 2.5 kHz is as follows: the measurement microphone is 74.2 dB; the smartphone is −61.5 dBFS. To confirm the stability of the application, the sound pressure at 1.0 kHz sine wave was measured after restarting the smartphone and application. **Table 2**

Table 2. Sound pressure at 1.0 kHz sine wave measured by smartphone microphone.

Count	Sound pressure [dBFS]
1	−42
2	−41
3	−42
4	−41
5	−41

Table 3. Sound pressure at each frequency.

Frequency [Hz]	Sound pressure	
	Microphone [dB]	Smartphone [dBFS]
125	77.3	−31.0
250	77.2	−29.0
500	77.3	−33.2
1000	77.2	−41.0
2000	77.2	−35.0
4000	77.2	−34.0
8000	77.2	−27.0
16000	77.2	−24.8

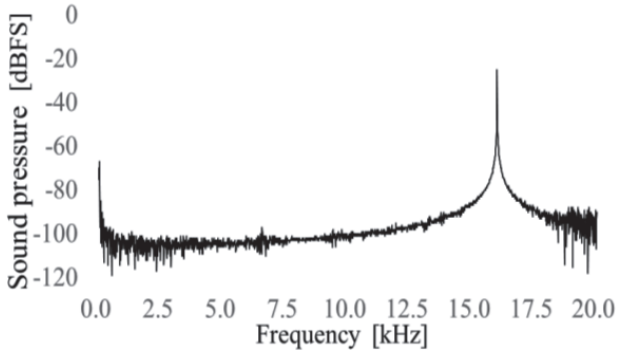

Fig. 3. Frequency spectrum chart of 16 kHz sine wave detected by smartphone microphone.

lists the sound pressures measured five times by the smartphone microphone. The sound pressures were −41 and −42 dBFS.

Next, the measured sound pressure for the center frequency of the octave band is shown in **Table 3**. These measurements eliminate the frequency dependence of the loudspeaker. The sound pressure of the measurement microphone was kept constant because there was no frequency dependence. The measurements of smartphone microphone is varied. The frequency spectrum chart of a sine wave at 16000 Hz is shown in **Fig. 3**. The peak frequency is 15999 Hz. As a result, we consider that the smartphone can be used for sound frequency analysis but not for absolute value measurement. If the measurement frequency is fixed, it is possible to make a relative comparison with the reference value.

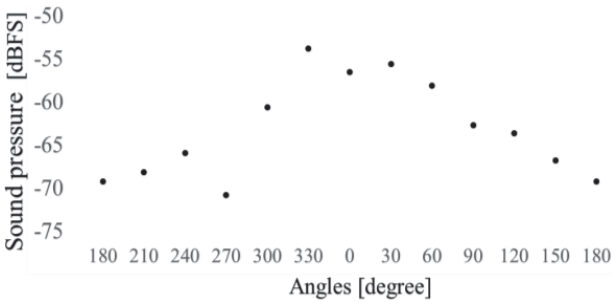

Fig. 4. Sound pressure at 16 kHz sine wave measured by smartphone microphone.

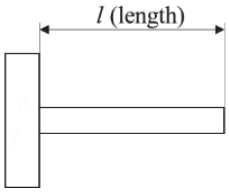

Fig. 5. Simple model of a cantilever beam.

2.3. Experimental Result of Directivity

Figure 4 shows a sound pressure at each angle measured by smartphone microphone. There was no difference in sound pressure in the range of 0°±30° . When shifted by more than 90°, the sound pressure decreased drastically. It can be seen that the sound is collected when the smartphone is within 0°±30° of the target.

3. Chattering Vibration Detection in the Presence of Environmental Noise

3.1. Theory

Chattering vibration is an abnormal vibration that tends to occur during the cutting process. In the chattering vibration state, the workpiece or tool rotates and deflects with a large amplitude [16–19, 21–23]. A simple model of a cantilever beam is shown in **Fig. 5**. The amount of deflection increases as the tool protrusion length increases and chattering vibration occurs.

3.2. Experimental Method

Figure 6 shows a schematic of the experimental setup for investigating cutting sounds. A lathe (HB-500 × 1000, Shoun Machine Tool Corp.) was utilized in the experiment because we did not have the single-purpose lathe. **Table 4** lists the experimental equipment and cutting conditions. The tool used was a boring tool (S16MSTFCR11, Mitsubishi Materials Corp.) and tip was cermet (TPGM110204L, Tungaloy Corp.), and the workpiece material is S55C. At the start of the experiment, the workpiece had a diameter of 34 mm and protrusion length of 67 mm. The aspect ratio was set to 2 for the workpiece. The tool protrusion length varied between 30 and 60 mm. The workpiece was cut from the edge to 25 mm, and the

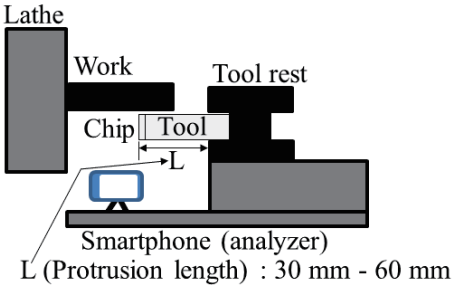

Fig. 6. Experimental setup.

Table 4. Cutting conditions.

Information	
Machine	Lathe
Cutting tool	Boring tools
Tip	Cermet
Workpiece material	S55C
Analyzer	Smartphone
Cutting conditions	
Rotational Speed	1150 min^{-1}
Feed	180 mm/min
Depth of cut	0.3 mm
Coolant	Non (dry)

cutting time was set to 8 seconds. The depth of cut was approximately 0.3 mm. The cutting sound was measured by smartphone. The smartphone moved synchronously with the tool rest. The cutting sound was FFT analyzed using a custom-made Android OS application for smartphone. FFT conditions are listed in **Table 1**. The sound pressure values after the FFT were saved in a csv file and the values were analyzed.

3.3. Experimental Results

We first evaluated the change in the sound pressure at 30 mm protrusion length of the tool. **Fig. 7(a)** shows a frequency spectrum chart of the average of the sound pressures during the cutting process. The cutting process time was approximately 8 seconds. The sound pressure at 6.5–9.0 kHz, 11.0–12.0 kHz, and 13.0–17.0 kHz increased. The sound pressure at 8677 Hz in the 5.0–10.0 kHz range and at 16149 Hz in the 10.0–19.0 kHz range increased the most. **Fig. 7(b)** compares the sound pressures of the average and 2 seconds after cutting start. The average sound pressure and the sound pressure after 2 seconds were inconsistent, and the frequency spectrum chart was unstable during the cutting process. A time series variation of the sound pressure at 8.7 kHz and 16.1 kHz are shown in **Fig. 8(a)** and **(b)**, respectively, indicating that the sound pressure is not constant. The maximum sound pressure at 8.7 kHz before cutting state is −71 dBFS, and the minimum sound pressure during cutting is −81 dBFS, which is less than the maximum value for the before cutting state. At 16.1 kHz, the maximum sound pressure before cutting state is −70 dBFS, and the minimum sound pressure during cutting is −82 dBFS. **Fig. 8(c)** shows the time variation of the feature value. The feature value is summed value of sound value for frequencies from 6.5–9.0 kHz. In this paper, the sound value is the sound pressure normalized with 0 dBFS as the maximum sound pressure value. For example, if the sound pressure at 8.7 kHz is −81 dBFS, the sound value at 8.7 kHz is −81. The maximum feature value before cutting state is −17043, and the minimum feature value during cutting is −16919. For the difference between the maximum sound pressure before cutting state and the minimum sound pressure during cutting, whereas the value at 8.4 kHz and 16.1 kHz were negative, the feature value of 6.5–9.0 kHz achieved 124. **Fig. 8(d)** shows the time variation of the sum of the sound value for frequencies from 13.0 kHz to 17.0 kHz. The maximum value before cutting state is −29414, and the minimum value during cutting is −28663, a difference of 751. This differential value is higher than the feature value of 6.5–9.0 kHz. From the comparison between them, we confirmed the effectiveness of summing sound value of 13.0–17.0 kHz because there is always a difference in value, and it is possible to distinguish between before cutting state and cutting state.

Next, the cutting for the protrusion length of the tool was varied from 30 mm to 40 mm, 50 mm, and 60 mm. Chattering vibration occurred at protrusion lengths of 50 mm and 60 mm. **Fig. 9(a)** shows the frequency spectrum chart at the 50 mm protrusion length of the tool. The sound pressure at approximately 3.5 kHz increases compared to the sound pressure at 30 mm protrusion length of the tool. **Table 5** shows the sum of the sound value for frequencies from 13.0 to 17.0 kHz (summation value). The summation value at a protrusion length of 40 mm was −27115, which was not different from that at 30 mm. The summation value at 50 mm protrusion length was −25587, an increase compared to that at 30 mm. The summation value at 60 mm protrusion length was −27900, a decrease compared to that at 30 mm. These data represent the averages of several experimental results. The standard deviations are listed in **Table 5**. Thus, the chattering vibration for a tool protrusion length of 50 mm can be distinguished using the smartphone by identifying the maximum summation value.

Figure 9(b) shows the frequency spectrum chart for a 60 mm protrusion length of the tool. The sound pressures at approximately 2.5 kHz and the harmonic components at approximately 2.5 kHz increases compared to the sound pressure at 30 mm protrusion length of the tool, indicating the occurrence of strong chattering vibration. The maximum sound pressure in the 0–10.0 kHz range was −35.7 dBFS, and the frequency of that sound pressure was approximately 2.5 kHz. The maximum sound pressure in the 10.0–20.0 kHz range was −43.7 dBFS, and the frequency of that sound pressure was approximately 12.4 kHz. For the cases of 30 mm and 60 mm protrusion length of the tool, **Table 6** lists the maximum sound pressure from 10.0 kHz to 20.0 kHz at 2.0 kHz intervals. The maximum sound pressure at 60 mm protrusion length of the tool in the 12.0–13.9 kHz range is −43.7 dBFS, and in the 14.0–15.9 kHz range is −50.6 dBFS. These values

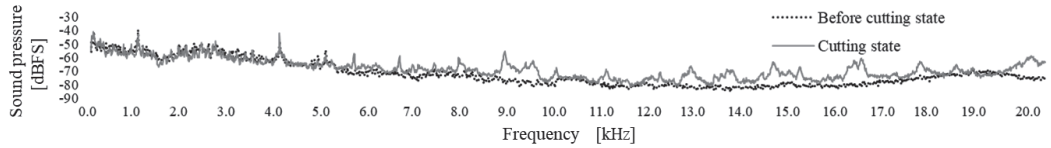

(a) Frequency spectrum chart of average cutting sound during cutting time

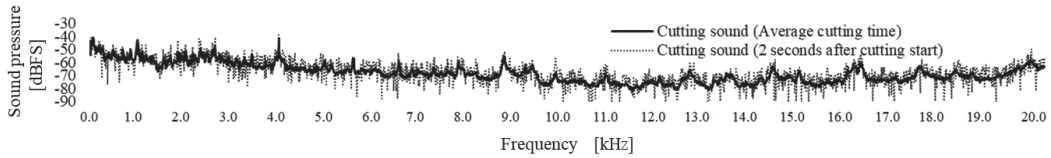

(b) Frequency spectrum chart of the average during cutting time and 2 seconds after the start of cutting

Fig. 7. Sound pressures at 30 mm protrusion length of the tool.

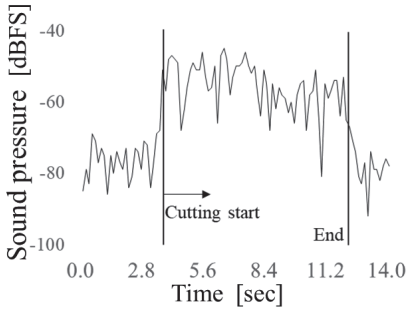

(a) Sound pressure at 8.7 kHz

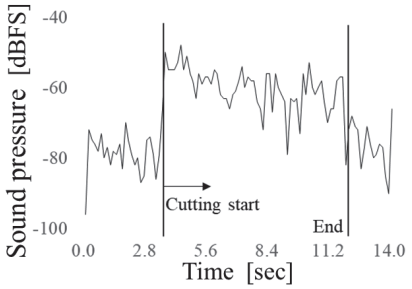

(b) Sound pressure at 16.1 kHz

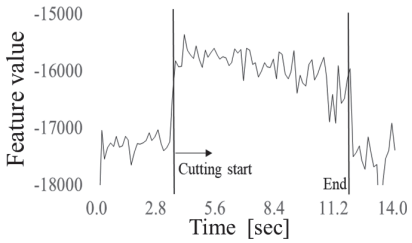

(c) Sum of sound value for frequencies from 6.5–9.0 kHz

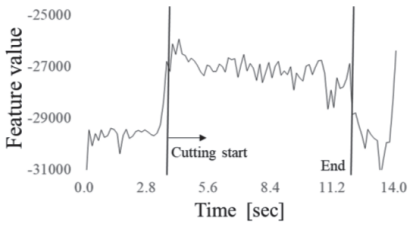

(d) Sum of sound value for frequencies from 13.0–17.0 kHz

Fig. 8. Time variation of sound pressure at 30 mm protrusion length of tool.

increased by more than 10 dB compared with the value of the 30 mm protrusion length of the tool. Thus, the chattering vibration for the tool protrusion length is 60 mm, which can be distinguished with the smartphone by identifying the maximum sound pressure between 10.0 kHz and 20.0 kHz.

3.4. Evaluation of Applications for Chattering Vibration Detection

In the previous section, we described how chattering vibrations could be detected by comparing the sound pressure with a tool protrusion length of 30 mm. In this section, we confirm the operating principle using CVDA. First, we performed cutting experiments at 30 mm protrusion length of the tool on multiple days, and calculated the average and standard deviation (σ) of the sound pressures. The reference range was defined as the average value $\pm 2\sigma$; the reference values are listed in **Table 7**.

Figure 10 shows a schematic of the experimental setup. The setup is essentially the same as in **Fig. 6**. In the first experiment, cutting was performed with 50 mm and 60 mm protrusion length of the tool in presence of non-noise. The operational results of CVDA are shown in **Tables 8** and **9**. Both sets of test data accurately determined chattering vibrations.

In the second experiment, cutting was performed with a 50 mm protrusion length of the tool in the presence of environmental noise. The setup is shown in **Fig. 10**. The smartphone2 (Rog Phone 5s, ASUSTeK Computer Inc.) was used to broadcast noise sounds during the cutting process. In some factories in Japan, school chimes are used to signal break time. The experiment was conducted under the assumption that the break time signal was played during cutting. The frequency spectrum chart of the school chime sound is shown in **Fig. 11**. The sound pressures below 5 kHz are increased. The cutting sound pressure between 0 kHz and 5 kHz at 50 mm protrusion length of the tool is shown in **Fig. 12**. Unlike the previous experimental results, the sound pressure was higher at 780 Hz and 2.0 kHz owing to the school chime sound. The sound pressure at 780 Hz and 2.0 kHz was −40 dBFS and −45 dBFS, respectively, both of which increased compared to the case of the 30 mm protrusion length of the tool. Next,

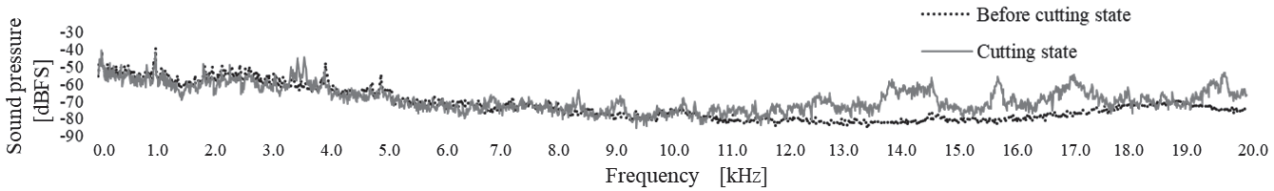

(a) Frequency spectrum chart at 50 mm protrusion length of the tool

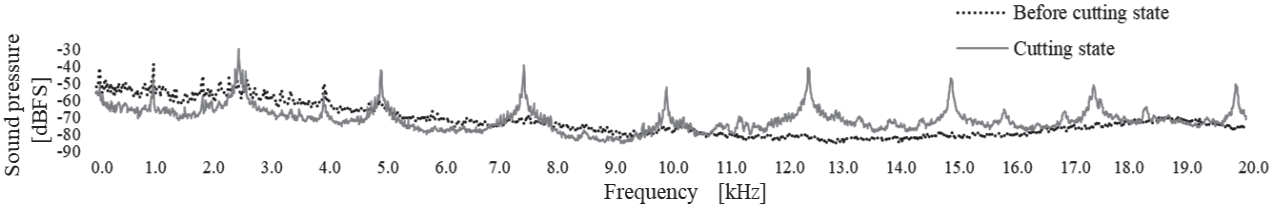

(b) Frequency spectrum chart at 60 mm protrusion length of the tool

Fig. 9. Frequency spectrum chart of average cutting sound during cutting time.

Table 5. Transition of summation value.

Protrusion length [mm]	Summation value	
	Average	Standard deviation (σ)
30	−27099	270
40	−27115	229
50	−25587	249
60	−27900	290

Table 6. Maximun sound pressure between 10 kHz and 20 kHz with tool protrusion lengths of 30 mm and 60 mm.

Frequency	Maximum sound pressure [dBFS]	
	30 mm protrusion length	60 mm protrusion length
10 kHz–11.9 kHz	−68.7	−70.7
12 kHz–13.9 kHz	−66.3	−43.7
14 kHz–15.9 kHz	−62.4	−50.6
16 kHz–17.9 kHz	−60.4	−53.6
18 kHz–20.0 kHz	−58.9	−52.8

Table 7. Reference value.

Frequency	Reference range
Summation value	−26560 to −27639
10 kHz–11.9 kHz	−86.5 to −56.1 dBFS
12 kHz–13.9 kHz	−76.0 to −62.8 dBFS
14 kHz–15.9 kHz	−73.4 to −61.3 dBFS
16 kHz–17.9 kHz	−67.4 to −60.1 dBFS
18 kHz–20.0 kHz	−45.9 to −75.9 dBFS

the change in the sound pressure of sound signals above 10 kHz is discussed. Five cuts were performed at 50 mm protrusion length of the tool, and the test results are listed in **Table 10**. The summation values were higher than the reference values, and the test results were all chattering vibration states. The differences between these experimental data and the values at 50 mm protrusion length of the

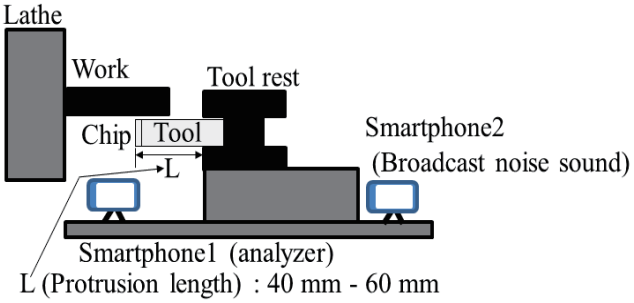

Fig. 10. Experimental setup for confirmation of the principle of chattering vibration detection in the presence of noise.

Table 8. Test results at 50 mm protrusion length of the tool in the presence of non-noise.

Count	Summation value	Test result
1	−25605	Chattering vibration
2	−26139	Chattering vibration
3	−25423	Chattering vibration
4	−25471	Chattering vibration
5	−25441	Chattering vibration

Table 9. Test results at 60 mm protrusion length of the tool in the presence of non-noise.

Count	Above 10 kHz		Test result
	Sound pressure [dBFS]	Frequency [kHz]	
1	−35.1	12.4	Chattering vibration
2	−45.6	12.8	Chattering vibration
3	−43.4	15.4	Chattering vibration
4	−56.7	15.3	Chattering vibration
5	−50.2	15.0	Chattering vibration

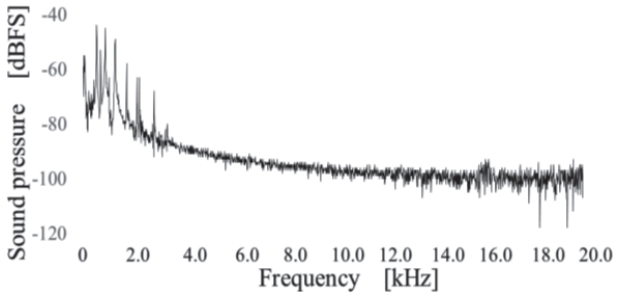

Fig. 11. Frequency spectrum chart of school chime.

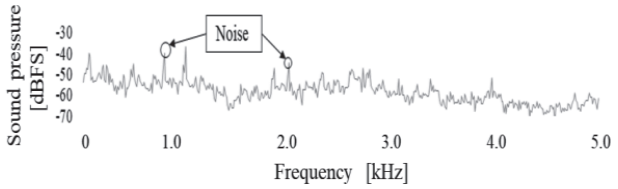

Fig. 12. Frequency spectrum chart of cutting sound of 0 Hz to 5 kHz at 50 mm protrusion length of the tool during a school chime broadcast.

Table 10. Test results at 50 mm protrusion length of the tool in the presence of school chime sound.

Count	Summation value	Test result
1	−26440	Chattering vibration
2	−25278	Chattering vibration
3	−24211	Chattering vibration
4	−24715	Chattering vibration
5	−25815	Chattering vibration

tool listed in **Table 5** are small. From the comparison, we confirmed the effectiveness of CVDA in the presence of environmental noise.

4. Chattering Vibration Detection in the Presence of Factory Noise

4.1. Chattering Vibration Detection Method

In the previous section, CVDA was assumed to be used for environmental noise between 0 Hz and 10 kHz. In this section, we consider the use of CVDA in an actual factory environment with various machine tool sounds between 0 Hz and 20 kHz. First, we recorded sound in an actual factory and analyzed the sound by FFT analysis in order to investigate the sound in the factory of a manufacturing company. **Fig. 13** shows the time variation of summation value, indicating that the sounds of various machine tool operations were included because the value was not constant.

We observed that it was possible to eliminate machine tool sounds outside of cutting time by collecting the sound during the cutting process. The tool rest of single-purpose lathe moved to the cutting position as cutting starts, and returns to the initial position when the cutting ends. We

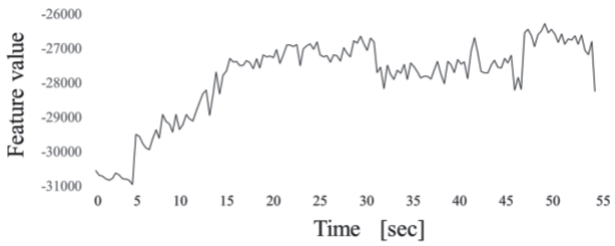

Fig. 13. Time variation of summation value in factory noise.

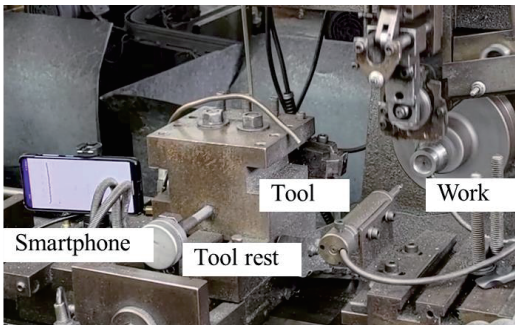

(a) Tool rest position is initial position

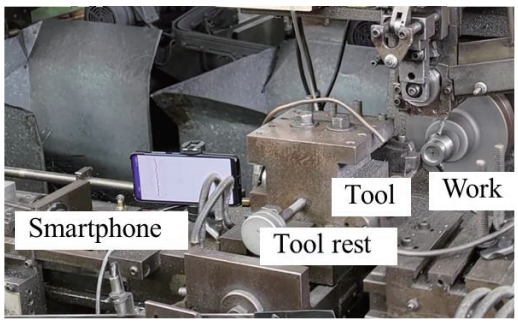

(b) Tool rest position is cutting position

Fig. 14. Experimental apparatus for detection of tool rest position by acceleration sensor of smartphone.

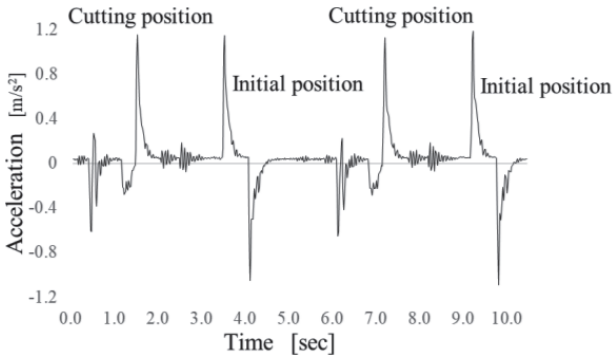

Fig. 15. Time variation of smartphone *Y*-axis acceleration sensor data.

investigated the relationship between tool rest motion and the accelerometer data of smartphone. **Fig. 14** shows the experimental apparatus in an actual factory. The single-purpose lathe moved automatically to the left and right while the cutting time remained constant. **Fig. 15** shows the time variation of *Y*-axis acceleration sensor data. The

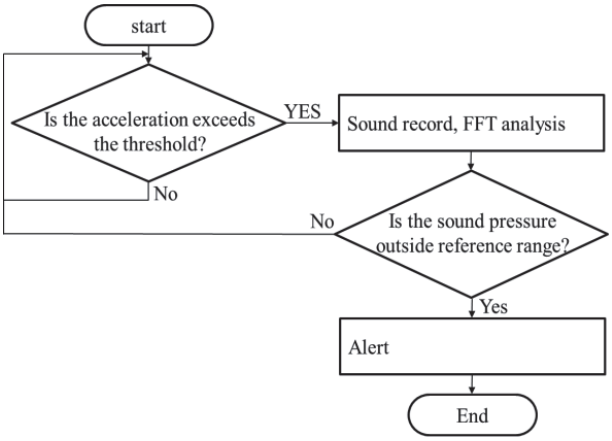

Fig. 16. Flow of chattering vibration detection.

time required to return to the initial position from the cutting position was consistent with the time interval at which the *Y*-axis acceleration sensor data exceeded 1.0 m/s^2. From the comparison between them, we confirmed the ability to determine the start and end timing of sound collection by using the acceleration sensor.

Figure 16 shows the flow of chattering vibration detection in the presence of factory noise. The configuration is simple and has a low CPU load because the CVDA does not require deep learning. Therefore, it can be used with the smartphone. Firstly, the acceleration sensor automatically detects the start time of cutting process. For the *Y*-axis acceleration sensor data, the threshold value is 1.0 m/s^2. As a result, the accuracy improved because the sound signals outside the cutting time were not analyzed. Secondly, the sound signals were analyzed and compared with the reference values. If the cutting sound was outside the reference range, it was judged as chattering vibration.

This application sends an e-mail to a worker when it detects chattering vibrations. The worker notices the chattering vibrations even if the worker is working far away from the target machine. By customizing the application, it is also possible to send notifications in ways other than e-mail.

4.2. Evaluation of Applications for Chattering Vibration Detection in the Presence of Factory Noise

In this section, we compare the classical statistical method with the proposed method in the presence of factory noise. The experimental setup is shown in **Fig. 10**. The lathe was manually shifted to the left or right by approximately 300 mm, adding an action that mimicked the motion of a single-purpose lathe. An experimental system was constructed to perform cutting 8 seconds after the acceleration sensor data response.

The cutting experiment was performed at 40 mm protrusion length of the tool in the presence of factory noise. **Fig. 17** shows the experimental results of the accelerometer data and summation value. The time at approximately 8 seconds after the acceleration sensor data response and the start time of the cutting process were almost the same. Seven seconds after the start of the cutting process, the sound pressure increased owing to factory noise. The method using only sound signals described in Sections 3.3 and 3.4 falsely detected the normal state as chattering vibration because the sound pressure at 17 kHz was −57 dBFS. The proposed method determined that it could be normal because it did not detect abnormal noise before the acceleration sensor reacts.

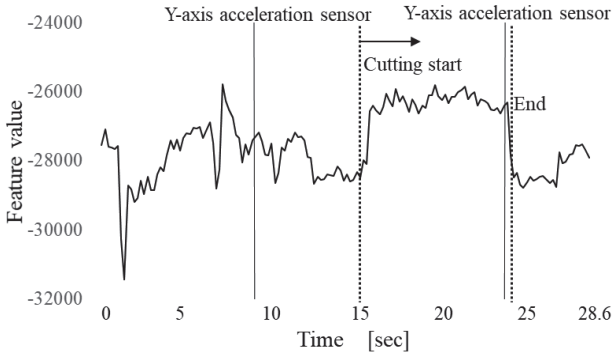

Fig. 17. Time variation of summation value at 40 mm protrusion length of the tool.

Table 11. Test results at 50 mm protrusion length of tool in presence of factory noise.

Count	Summation value	Test result
1	−25886	Chattering vibration
2	−26224	Chattering vibration
3	−26199	Chattering vibration
4	−25783	Chattering vibration
5	−25366	Chattering vibration
6	−25920	Chattering vibration
7	−26208	Chattering vibration
8	−25885	Chattering vibration
9	−26191	Chattering vibration
10	−25275	Chattering vibration

Next, a cutting experiment was conducted ten times with the protrusion length set to 50 mm in the presence of factory noise. The sound of the cutting timing assumed from the acceleration sensor was analyzed. The test results are listed in **Table 11**. The CVDA was determined to be in a state of chattering vibration.

5. Conclusions

The purpose of this study was to develop an inexpensive and high-accuracy smartphone application to detect chattering vibration in a single-purpose lathe. We focused on sound signals between 10 kHz and 20 kHz to improve accuracy, and investigated the relationship between sound pressure and chattering vibration. The relationship between the acceleration sensor and the operation of the single-purpose lathe was also investigated. As a result, the following con-

clusions were drawn.

(1) Chattering vibration occurred when the tool protrusion length was increased. The level of the sound signals between 10 kHz and 20 kHz increased when chattering vibration occurred. This can be explained by the fact that the tool vibration affected the sound signal above 10 kHz.

(2) In the experiment, the sound pressure at 6.5–9.0 kHz, 11.0–12.0 kHz, and 13.0–17.0 kHz increased with normal cutting. The summation value produced a difference before and during the cutting operation.

(3) The movement of the single-purpose lathe can be detected using an acceleration sensor. It was found that the timing of the start and end of the cutting process can be detected. As a result, the accuracy was improved by eliminating anomalous noise before the cutting process.

(4) The proposed method has a simple configuration and works on smartphones. The advantage of smartphones is that the number of devices can be reduced because they are equipped with sound sensors, acceleration sensors, camera functions, and a CPU as standard. In addition, they can easily be placed near the target machine because of their portability, and it is possible to accurately record the sound of the target machine. As a result, it could be used as a low-cost system.

In the proposed method, the threshold settings for the sound signals and accelerometer data are important, especially the reference range of the sound signal. However, this was not fully investigated in the present study. Detailed comparisons between measurements and smartphone microphones are also insufficient. We will further investigate the improvements in threshold settings and microphone characteristics in detail in future work. In addition, if the cutting conditions change, the reference value must also be modified. Methods for easily modifying reference values is another issue for the future.

Acknowledgments

Special thanks to Mr. Okazaki of section manager in Yata Manufacturing Corporation.

References:

[1] T. Yamamoto, R. Matsuda, M. Shindou, T. Hirogaki, and E. Aoyama, "Monitoring of vibrations in free-form surface processing using ball nose end mill tools with wireless tool holder systems," Int. J. Automation Technol., Vol.15, No.3, pp. 335-342, 2021. https://doi.org/10.20965/ijat.2021.p0335

[2] A. Hayashi, O. Shibata, and Y. Morimoto, "Study on method for avoiding chatter vibration by changing machine tool rigidity," Int. J. Automation Technol., Vol.16, No.6, pp. 853-861, 2022. https://doi.org/10.20965/ijat.2022.p0853

[3] L. Lu, M. Sato, and H. Tanaka, "Experimental verification of chatter-free ball end milling strategy," Int. J. Automation Technol., Vol.7, No.1, pp. 45-51, 2013. https://doi.org/10.20965/ijat.2013.p0045

[4] C. Sun and Y. Altintas, "Chatter free tool orientations in 5-axis ball-end milling," Int. J. of Machine Tools and Manufacture, Vol.106, pp. 89-97, 2016. https://doi.org/10.1016/j.ijmachtools.2016.04.007

[5] R. Matsuda, M. Shindou, T. Hirogaki, and E. Aoyama, "Monitoring of rotational vibration in tap and endmill processes with a wireless multifunctional tool holder system," Int. J. Automation Technol., Vol.12, No.6, pp. 876-882, 2018. https://doi.org/10.20965/ijat.2018.p0876

[6] J. Slavicek, "The effect of irregular tooth pitch on stability of milling," Proc. 6th Int. MTDR Conf., pp. 15-22, 1965.

[7] T. Atsuta, H. Yoshimura, and T. Matsumura, "Inner modulation controlled process for suppression of chatter vibration in double inserts turning," Int. J. Automation Technol., Vol.18, No.3, pp. 374-381, 2024. https://doi.org/10.20965/ijat.2024.p0374

[8] H. Cao, Y. Yue, X. Chen, and X. Zhang, "Chatter detection in milling process based on synchrosqueezing transform of sound signals," Int. J. Adv. Manuf. Technol., Vol.89, pp. 2747-2755, 2016. https://doi.org/10.1007/s00170-016-9660-7

[9] R. Ichimiya, K. Chiku, and M. Aichi, "Analyses of noise emitted in cutting operation (1st report) – Sound pressure level in metal cutting with a single point cutting tool –," J. Jpn. Society for Precision Engineering, Vol.49, No.3, pp. 95-100, 1983 (in Japanese).

[10] H. Takahashi, K. Sakai, and H. Shizuka, "Development of an in situ tool wear monitoring system using the cutting sound," Advanced Materials Research, Vol.1117, pp. 277-280, 2015. https://doi.org/10.4028/www.scientific.net/AMR.1117.277

[11] H. Matsumoto and T. Kondo, "Study on distinction of cutting condition based on cutting sound – System development and examination –," JSME The Proc. of Conf. of Hokkaido Branch, Vol.46, No.408, pp. 109-110, 2007 (in Japanese). https://doi.org/10.1299/jsmehokkaido.2007.46.109

[12] X. Li, "A brief review: Acoustic emission method for tool wear monitoring during turning," Int. J. of Machine Tools and Manufacture, Vol.42, No.2, pp. 157-165, 2002. https://doi.org/10.1016/S0890-6955(01)00108-0

[13] Y. Koizumi, S. Saito, H. Uematsu, Y. Kawachi, and N. Harada, "Unsupervised detection of anomalous sound based on deep learning and the Neyman–Pearson lemma," IEEE/ACM Trans. Audio, Speech, Language Process., Vol.27, No.1, pp. 212-224, 2019. https://doi.org/10.1109/TASLP.2018.2877258

[14] A. Aiba, M. Yoshida, D. Kitamura, S. Tamamichi, and H. Haruwatari, "Noise robust acoustic anomaly detection system with nonnegative matrix factorization based on generalized gaussian distribution," IEICE Trans. Inf. & SYST., Vol.E104.D, No.3, pp. 441-449, 2021. https://doi.org/10.1587/transinf.2020EDK0002

[15] T. Nishida, K. Dohi, T. Endo, M. Yamamoto, and Y. Kawaguchi, "Anomalous sound detection based on machine activity detection," 2022 30th European Signal Processing Conf. (EUSIPCO), pp. 269-273, 2022.

[16] M. Honda and T. Yasui, "A study on the rigidity of machine tools," Trans. Jpn. Soc. Mechan. Eng., Vol.67, No.546, pp. 82-97, 1964 (in Japanese).

[17] Y. Kurita, Y. Oura, T. Tanaka, and M. Kawata, "Chatter vibration of workpiece deformation type in cutting thin-walled cylindrical workpiece (Generation mechanism of chatter vibration)," Trans. JSME, Vol.86, No.884, Article No.19-00335, 2020 (in Japanese). https://doi.org/10.1299/transjsme.19-00335

[18] E. Marui, S. Ema, and S. Kato, "Chatter vibration of lathe tools. Part 1: General characteristics of chatter vibration," J. Eng. Ind., Vol.105, pp. 100-106, 1983 (in Japanese). https://doi.org/10.1115/1.3185866

[19] E. Marui, "Chatter vibration of lathe tools, Part2: On the mechanism of exciting energy supply," J. Eng. Ind., Vol.105, pp. 107-113, 1983 (in Japanese). https://doi.org/10.1115/1.3185867

[20] U.S. Department of Labor: Occupational Safety and Health Administration, "Noise control: A guide for workers and employers," 1980.

[21] N. Suzuki, "Chatter vibration in cutting, part 1," J. Jpn. Society for Precision Engineering, Vol.76, No.3, pp. 280-284,2010 (in Japanese). https://doi.org/10.2493/jjspe.76.280

[22] N. Suzuki, "Chatter vibration in cutting, part 2," J. Jpn. Society for Precision Engineering, Vol.76, No.4, pp. 404-408, 2010 (in Japanese). https://doi.org/10.2493/jjspe.76.404

[23] Y. Altintas, E. Shamoto, P. Lee, and E. Budak, "Analytical prediction of stability lobes in ball end milling," ASME J. Manuf. Sci. Eng., Vol.121, No.4, 1999. https://doi.org/10.1115/1.2833064

Name:
Yoshihiro Makimoto

Affiliation:
Tokushima Prefectural Industrial Technology Center

Address:
11-2 Nishibari, Saika-cho, Tokushima, Tokushima 770-8021, Japan

Brief Biographical History:
2010- Engineer, Shikoku Electric Power Co., Inc.
2020- Engineer, Shikoku Electric Power Transmission & Distribution Co., Inc.
2021- Researcher, Tokushima Prefectural Industrial Technology Center
2022- Senior Researcher, Tokushima Prefectural Industrial Technology Center

Main Works:
• "Waveguide-type Optical Circuit for Recognition of Optical QPSK Coded Labels in Photonic Router," J. of Lightwave Technology, Vol.27, No.1, pp. 60-67, 2009.
• "Wavelength Dependence of Optical Waveguide-Type Devices for Recognition of QPSK Routing Labels," IEICE Trans. on Electronics, Vol.E-93-C, No.2, pp. 157-163, 2010.

Membership in Academic Societies:
• The Institute of Electronics, Information and Communication Engineers (IEICE)

Name:
Yuya Nara

Affiliation:
Tokushima Prefectural Industrial Technology Center

Address:
11-2 Nishibari, Saika-cho, Tokushima, Tokushima 770-8021, Japan

Brief Biographical History:
2019- Engineer, Panasonic Industrial Devices SUNX Kyushu Co., Ltd.
2020- Researcher, Tokushima Prefectural Industrial Technology Center
2022- Senior Researcher, Tokushima Prefectural Industrial Technology Center

Name:
Syuma Hirai

Affiliation:
Graduate School of Science and Technology, Tokushima University

Address:
2-1 Minamijosanjima-cho, Tokushima, Tokushima 770-8506, Japan

Membership in Academic Societies:
• The Japan Society for Precision Engineering (JSPE)

Name:
Akira Mizobuchi

ORCID:
0000-0003-4937-089X

Affiliation:
Associate Professor, Graduate School of Technology, Industrial and Social Sciences, Tokushima University

Address:
2-1 Minamijosanjima-cho, Tokushima, Tokushima 770-8506, Japan

Brief Biographical History:
1999- Research Associate, Tokushima University
2007- Assistant Professor, Tokushima University
2013- Associate Professor, Tokushima University

Main Works:
• "Slag Sticking Suppression in Gas Cutting of Steel Plate by Carbon-added Paste," J. of Japan Society for Design Engineering, Vol.55, No.11, pp. 673-680, 2020 (in Japanese).
• "Optimization of Wet Grinding Conditions of Sheets Made of Stainless Steel," J. of Manufacturing and Materials Processing, Vol.4, No.4, Article No.114, 2020.
• "Polishing Performance of a Recycled Grinding Wheel Using Grinding Wheel Scraps for the Wet Polishing of Stainless-Steel Sheets," Int. J. Automation Technol., Vol.16, No.1, pp. 60-70, 2022.

Membership in Academic Societies:
• The Japan Society of Mechanical Engineers (JSME)
• The Japan Society for Precision Engineering (JSPE)
• The Japan Society for Abrasive Technology (JSAT)
• The Japan Society of Electro-Machining Engineers (JSEME)
• Japan Society for Design Engineering (JSDE)

Name:
Yuki Oe

Affiliation:
Tokushima Prefectural Industrial Technology Center

Address:
11-2 Nishibari, Saika-cho, Tokushima, Tokushima 770-8021, Japan

Brief Biographical History:
2013- Engineer, Nissan Motor Co., Ltd.
2017- Researcher, Tokushima Prefectural Industrial Technology Center
2021- Senior Researcher, Tokushima Prefectural Industrial Technology Center

Membership in Academic Societies:
• Acoustical Society of Japan (ASJ)
• Japan Human Factors and Ergonomics Society (JES)
• Japan Society of Kansei Engineering (JSKE)

Name:
Hitoshi Ogawa

Affiliation:
Tokushima Prefectural Industrial Technology Center

Address:
11-2 Nishibari, Saika-cho, Tokushima, Tokushima 770-8021, Japan

Brief Biographical History:
1998- Researcher, Tokushima Prefectural Industrial Technology Center
2007- Senior Researcher, Tokushima Prefectural Industrial Technology Center
2020- Team Leader, Tokushima Prefectural Industrial Technology Center

Main Works:
• "Effect of Cavitation of Cutting Fluid in Micro Drilling (1st Report)—Researches on Applying Ultrasonic Vibration on Machining Fluid—," J. Jpn. Society for Precision Engineering, Vol.72, No.5, pp. 626-630, 2006 (in Japanese).
• "Relation between Drilling Conditions and Tool Life in Micro Drilling (2nd Report)—Researches on Applying Ultrasonic Vibration on Machining Fluid—," J. Jpn. Society for Precision Engineering, Vol.73, No.5, pp. 578-582, 2007 (in Japanese).
• "Effects of Cavitation on Burr and Tool Life in Micro Through Hole Drilling (3rd Report)—Researches on Applying Ultrasonic Vibration on Machining Fluid—," J. Jpn. Society for Precision Engineering, Vol.74, No.10, pp. 1092-1096, 2008 (in Japanese).

Membership in Academic Societies:
• The Japan Society for Precision Engineering (JSPE)
• The Japan Society of Electro-Machining Engineers (JSEME)